PERGAMON

International Journal of Solids and Structures 38 (2001) 7703–7721

INTERNATIONAL JOURNAL OF SOLIDS and STRUCTURES

www.elsevier.com/locate/ijsolstr

Postbuckling of shear deformable laminated plates with piezoelectric actuators under complex loading conditions

Hui-Shen Shen

School of Civil Engineering and Mechanics, Shanghai Jiao Tong University, 1954 Hua Shan Road, Shanghai 200030, China

Received 24 January 2001; in revised form 10 May 2001

Abstract

Postbuckling analysis is presented for a simply supported, shear deformable laminated plate with piezoelectric actuators subjected to the combined action of mechanical, electric and thermal loads. The temperature field considered is assumed to be a uniform distribution over the plate surface and through the plate thickness and the electric field is assumed to be the transverse component E_Z only. The material properties are assumed to be independent of the temperature and the electric field. The governing equations of a laminated plate are based on Reddy's higher order shear deformation plate theory that includes thermo-piezoelectric effects. The initial geometric imperfection of the plate is taken into account. Two cases of the in-plane boundary conditions are considered. A perturbation technique is employed to determine buckling loads and postbuckling equilibrium paths. The numerical illustrations concern the postbuckling behavior of perfect and imperfect, symmetric cross-ply and antisymmetric angle-ply laminated plates with fully covered or embedded piezoelectric actuators under different sets of thermal and electric loading conditions. The effects played by temperature rise, applied voltage, the character of in-plane boundary conditions, transverse shear deformation, plate aspect ratio, fiber orientation and stacking sequence as well as initial geometric imperfections are studied.

Keywords: Postbuckling; Laminates; Thermo-piezoelectric effect; Higher order shear deformation plate theory; Perturbation technique

1. Introduction

One of the recent advances in material and structural engineering is in the field of smart structures which incorporates adaptive materials. By taking advantage of the direct and converse piezoelectric effects, piezoelectric composite structures can combine the traditional performance advantages of composite laminates along with the inherent capability of piezoelectric materials to adapt to their current environment. Therefore, hybrid laminated structures where a substrate made laminated material is coupled with surface-bonded or embedded piezoelectric actuator and/or sensor layers are becoming increasingly important.

E-mail address: hsshen@mail.sjtu.edu.cn (H.-S. Shen).

0020-7683/01/$ - see front matter
PII: S0020-7683(01)00120-2

Many postbuckling studies of composite laminated plates subjected to mechanical and thermal loading are available in the literature, see, for example, Noor and Peters (1992, 1994), Noor et al. (1993), Librescu and Souza (1993), Librescu et al. (1995), Argyris and Tenek (1995), and Shen (1988, 2000c). However, relatively few have been made on the coupled mechanical, electrical and thermal response of laminated composite plates containing piezoelectric layers. Tauchert (1992) gave an analytical solution for hybrid plates based on classical laminated plate theory. Jonnalagadda et al. (1994) employed first-order shear deformation plate theory to solve the piezothermoelastic response of hybrid plates and gave a Navier-type solution. Xu et al. (1995) gave the exact, three-dimensional piezothermoelastic solution of simply supported rectangular hybrid plates. Kapuria et al. (1997) gave a Levy-type solution for hybrid plates with various boundary conditions. Lee and Saravanos (1997) examined static bending and twisting responses of hybrid plates in thermal environments. Reddy (1999) gave the Navier solutions and finite element models based on the classical and shear deformation plate theories for laminated composite plates integrated sensors and/or actuators and subjected to mechanical, electrical and thermal loads. Ishihara and Noda (2000) studied the piezoelectric and pyroelectric effects on the linear response of hybrid plates subjected to mechanical, electrical and thermal loads. However, published literature on the nonlinear response of smart structures is limited in number. Icardi and Di Sciuva (1996) analyzed cross-ply laminated plates with top and bottom actuators under transverse distributed loads and large deflection conditions, but their numerical results were only for a simple case of cylindrical bending. Oh et al. (2000) studied thermal postbuckling behavior of laminated plates with top and/or bottom actuators subjected to thermal and electric loads. In their analysis nonlinear finite element equations based on layerwise displacement theory were formulated, but their numerical results were only for thin plates and all plates were assumed to have perfect initial configurations. To the best of the author's knowledge, there is no literature covering postbuckling response of imperfect shear deformable laminated plates with piezoelectric layers subjected to the combined action of mechanical, electric and thermal loads. This is the problem studied in the present paper, for the case when all four edges of the plate are assumed to be simply supported.

In the present study, the temperature field considered is assumed to be a uniform distribution over the plate surface and through the plate thickness. The electric field is assumed to be the transverse component E_Z only. The material properties are assumed to be independent of the temperature and the electric field. The governing equations of the plate are based on Reddy's (1999) higher order shear deformation plate theory (HSDPT) that includes thermo-piezoelectric effects. The initial geometric imperfection of the plate is taken into account but, for simplicity, its form is assumed to be the same as the initial buckling mode of the plate. Two cases of the in-plane boundary conditions are considered. A perturbation technique is employed to determine buckling loads and postbuckling equilibrium paths. Extensive numerical results are presented showing the effects of variation in the load parameters and geometric parameters of the plate on the different response characteristics.

2. Theoretical development

Consider a rectangular plate of length a, width b and constant thickness t, which consists of N plies, simply supported at four edges. The plate is subjected to a compressive edge load P in the X-direction combined with thermal and electric loads. As usual, the coordinate system has its origin at the corner of the plate. Let $\overline{U}$, $\overline{V}$ and $\overline{W}$ be the plate displacements parallel to a right-hand set of axes (X, Y, Z), where X is longitudinal and Z is perpendicular to the plate. $\overline{\Psi}_x$ and $\overline{\Psi}_y$ are the mid-plane rotations of the normals about the Y- and X-axes, respectively. Denoting the initial geometric imperfection by $\overline{W}^*(X, Y)$, let $\overline{W}(X, Y)$ be the additional deflection and $\overline{F}(X, Y)$ be the stress function for the stress resultants defined by $\overline{N}_x = \overline{F}_{,yy}$, $\overline{N}_y = \overline{F}_{,xx}$ and $\overline{N}_{xy} = -\overline{F}_{,xy}$, where a comma denotes partial differentiation with respect to the corresponding coordinates.

Attention is confined to two cases: (1) symmetric cross-ply laminated plates, and (2) antisymmetric angle-ply laminated plates with symmetrically fully covered or embedded piezoelectric actuators. Note that, for case (2) now the plate stiffnesses D_{16}, D_{26}, A_{16} and A_{26} do not equal to zero exactly, and the results are only approximate.

Reddy (1984) developed a simple HSDPT, in which the transverse shear strains are assumed to be parabolically distributed across the plate thickness and which contains the same dependent unknowns as in the first order shear deformation theory. From Reddy's HSDPT and including thermo-piezoelectric effects, the governing differential equations are

$$\widetilde{L}_{11}(\overline{W}) - \widetilde{L}_{12}(\overline{\Psi}_x) - \widetilde{L}_{13}(\overline{\Psi}_y) + \widetilde{L}_{14}(\overline{F}) - \widetilde{L}_{15}(\overline{N}^p) - \widetilde{L}_{16}(\overline{M}^p) = \widetilde{L}(\overline{W} + \overline{W}^*, \overline{F}) \tag{1}$$

$$\widetilde{L}_{21}(\overline{F}) + \widetilde{L}_{22}(\overline{\Psi}_x) + \widetilde{L}_{23}(\overline{\Psi}_y) - \widetilde{L}_{24}(\overline{W}) - \widetilde{L}_{25}(\overline{N}^p) = -\frac{1}{2}\widetilde{L}(\overline{W} + 2\overline{W}^*, \overline{W}) \tag{2}$$

$$\widetilde{L}_{31}(\overline{W}) + \widetilde{L}_{32}(\overline{\Psi}_x) - \widetilde{L}_{33}(\overline{\Psi}_y) + \widetilde{L}_{34}(\overline{F}) - \widetilde{L}_{35}(\overline{N}^p) - \widetilde{L}_{36}(\overline{S}^p) = 0 \tag{3}$$

$$\widetilde{L}_{41}(\overline{W}) - \widetilde{L}_{42}(\overline{\Psi}_x) + \widetilde{L}_{43}(\overline{\Psi}_y) + \widetilde{L}_{44}(\overline{F}) - \widetilde{L}_{45}(\overline{N}^p) - \widetilde{L}_{46}(\overline{S}^p) = 0 \tag{4}$$

where linear operators $\widetilde{L}_{ij}(\ )$ and nonlinear operator $\widetilde{L}(\ )$ are defined as in Appendix A.

It is noted that these plate equations show thermo-piezoelectric coupling as well as the interaction of stretching and bending.

All four edges are assumed to be simply supported. Depending upon the in-plane behavior at the edges, two cases will be considered.

Case (1): The edges are simply supported and freely movable in the X- and Y-directions, respectively.

Case (2): All four edges are simply supported. Uniaxial edge loads are acting in the X-direction. The edges $X = 0$, a are considered freely movable (in the in-plane direction), the remaining two edges being unloaded and immovable (in the Y-direction).

For both cases the associated boundary conditions could be found in Librescu and Stein (1991) and Shen and Zhang (1988). In the present paper, they are

$X = 0$, a:

$$\overline{W} = \overline{\Psi}_y = 0 \tag{5a}$$

$$\overline{N}_{xy} = 0, \quad \overline{M}_x = \overline{P}_x = 0 \tag{5b}$$

$$\int_0^b \overline{N}_x \, \mathrm{d}Y + P = 0 \tag{5c}$$

$Y = 0$, b:

$$\overline{W} = \overline{\Psi}_x = 0 \tag{5d}$$

$$\overline{N}_{xy} = 0, \quad \overline{M}_y = \overline{P}_y = 0 \tag{5e}$$

$$\int_0^a \overline{N}_y \, \mathrm{d}X = 0 \quad \text{(movable edges)} \tag{5f}$$

$$\overline{V} = 0 \quad \text{(immovable edges)} \tag{5g}$$

where $\overline{M}_x$ and $\overline{M}_y$ are the bending moments and $\overline{P}_x$ and $\overline{P}_y$ are the higher order moments as defined in Reddy (1984).

The condition expressing the immovability condition $\overline{V}=0$ (on $Y=0,\ b$) is fulfilled on the average senses as (Librescu et al., 1995; Shen, 2000b)

$$\int_0^a \int_0^b \frac{\partial \overline{V}}{\partial Y}\,\mathrm{d}Y\,\mathrm{d}X = 0 \tag{5h}$$

This condition in conjunction with Eq. (6b) below provides the compressive stresses acting on the edges $Y=0,\ b$.

The average end-shortening relationships are

$$\begin{aligned}\frac{\Delta_x}{a} &= -\frac{1}{ab}\int_0^b \int_0^a \frac{\partial \overline{U}}{\partial X}\,\mathrm{d}X\,\mathrm{d}Y \\ &= -\frac{1}{ab}\int_0^b \int_0^a \left\{ \left[A_{11}^* \frac{\partial^2 \overline{F}}{\partial Y^2} + A_{12}^* \frac{\partial^2 \overline{F}}{\partial X^2} + \left(B_{16}^* - \frac{4}{3t^2} E_{16}^* \right) \left(\frac{\partial \overline{\Psi}_x}{\partial Y} + \frac{\partial \overline{\Psi}_y}{\partial X} \right) - \frac{8}{3t^2} E_{16}^* \frac{\partial^2 \overline{W}}{\partial X\,\partial Y} \right] \right. \\ &\quad \left. - \frac{1}{2}\left(\frac{\partial \overline{W}}{\partial X} \right)^2 - \frac{\partial \overline{W}}{\partial X}\frac{\partial \overline{W}^*}{\partial X} - \left(A_{11}^* \overline{N}_x^P + A_{12}^* \overline{N}_y^P \right) \right\} \mathrm{d}X\,\mathrm{d}Y \end{aligned} \tag{6a}$$

$$\begin{aligned}\frac{\Delta_y}{b} &= -\frac{1}{ab}\int_0^a \int_0^b \frac{\partial \overline{V}}{\partial Y}\,\mathrm{d}Y\,\mathrm{d}X \\ &= -\frac{1}{ab}\int_0^a \int_0^b \left\{ \left[A_{22}^* \frac{\partial^2 \overline{F}}{\partial X^2} + A_{12}^* \frac{\partial^2 \overline{F}}{\partial Y^2} + \left(B_{26}^* - \frac{4}{3t^2} E_{26}^* \right) \left(\frac{\partial \overline{\Psi}_x}{\partial Y} + \frac{\partial \overline{\Psi}_y}{\partial X} \right) - \frac{8}{3t^2} E_{26}^* \frac{\partial^2 \overline{W}}{\partial X\,\partial Y} \right] \right. \\ &\quad \left. - \frac{1}{2}\left(\frac{\partial \overline{W}}{\partial Y} \right)^2 - \frac{\partial \overline{W}}{\partial Y}\frac{\partial \overline{W}^*}{\partial Y} - \left(A_{12}^* \overline{N}_x^P + A_{22}^* \overline{N}_y^P \right) \right\} \mathrm{d}Y\,\mathrm{d}X \end{aligned} \tag{6b}$$

where Δ_x and Δ_y are plate end-shortening displacements in the X- and Y-directions.

The temperature field is assumed to be a uniform distribution over the plate surface and through the plate thickness.

For the plate type piezoelectric material, only thickness direction electric field E_Z is dominant, and it is assumed that

$$E_Z = \frac{V_k}{t_k} \tag{7}$$

where V_k is the applied voltage across the kth ply and t_k is the thickness of the ply.

The equivalent thermo-piezoelectric loads are defined as

$$\begin{bmatrix} \overline{N}^P \\ \overline{M}^P \\ \overline{S}^P \end{bmatrix} = \begin{bmatrix} \overline{N}^T \\ \overline{M}^T \\ \overline{S}^T \end{bmatrix} + \begin{bmatrix} \overline{N}^E \\ \overline{M}^E \\ \overline{S}^E \end{bmatrix} \tag{8}$$

The forces, moments and higher order moments caused by elevated temperature or electric field are defined by

$$\begin{bmatrix} \overline{N}_x^T & \overline{M}_x^T & \overline{P}_x^T \\ \overline{N}_y^T & \overline{M}_y^T & \overline{P}_y^T \\ \overline{N}_{xy}^T & \overline{M}_{xy}^T & \overline{P}_{xy}^T \end{bmatrix} = \sum_{k=1}^{N} \int_{t_{k-1}}^{t_k} (1, Z, Z^3) \begin{bmatrix} A_x \\ A_y \\ A_{xy} \end{bmatrix}_k \Delta T\,\mathrm{d}Z \tag{9a}$$

$$\begin{bmatrix} \overline{S}_x^T \\ \overline{S}_y^T \\ \overline{S}_{xy}^T \end{bmatrix} = \begin{bmatrix} \overline{M}_x^T \\ \overline{M}_y^T \\ \overline{M}_{xy}^T \end{bmatrix} - \frac{4}{3t^2} \begin{bmatrix} \overline{P}_x^T \\ \overline{P}_y^T \\ \overline{P}_{xy}^T \end{bmatrix} \tag{9b}$$

or

$$\begin{bmatrix} \overline{N}_x^E & \overline{M}_x^E & \overline{P}_x^E \\ \overline{N}_y^E & \overline{M}_y^E & \overline{P}_y^E \\ \overline{N}_{xy}^E & \overline{M}_{xy}^E & \overline{P}_{xy}^E \end{bmatrix} = \sum_{k=1}^{N} \int_{t_{k-1}}^{t_k} (1, Z, Z^3) \begin{bmatrix} B_x \\ B_y \\ B_{xy} \end{bmatrix}_k \frac{V_k}{t_k} \, \mathrm{d}Z \tag{9c}$$

$$\begin{bmatrix} \overline{S}_x^E \\ \overline{S}_y^E \\ \overline{S}_{xy}^E \end{bmatrix} = \begin{bmatrix} \overline{M}_x^E \\ \overline{M}_y^E \\ \overline{M}_{xy}^E \end{bmatrix} - \frac{4}{3t^2} \begin{bmatrix} \overline{P}_x^E \\ \overline{P}_y^E \\ \overline{P}_{xy}^E \end{bmatrix} \tag{9d}$$

and

$$\begin{bmatrix} A_x \\ A_y \\ A_{xy} \end{bmatrix} = - \begin{bmatrix} \overline{Q}_{11} & \overline{Q}_{12} & \overline{Q}_{16} \\ \overline{Q}_{12} & \overline{Q}_{22} & \overline{Q}_{26} \\ \overline{Q}_{16} & \overline{Q}_{26} & \overline{Q}_{66} \end{bmatrix} \begin{bmatrix} c^2 & s^2 \\ s^2 & c^2 \\ 2cs & -2cs \end{bmatrix} \begin{bmatrix} \alpha_{11} \\ \alpha_{22} \end{bmatrix} \tag{10a}$$

$$\begin{bmatrix} B_x \\ B_y \\ B_{xy} \end{bmatrix} = - \begin{bmatrix} \overline{Q}_{11} & \overline{Q}_{12} & \overline{Q}_{16} \\ \overline{Q}_{12} & \overline{Q}_{22} & \overline{Q}_{26} \\ \overline{Q}_{16} & \overline{Q}_{26} & \overline{Q}_{66} \end{bmatrix} \begin{bmatrix} c^2 & s^2 \\ s^2 & c^2 \\ 2cs & -2cs \end{bmatrix} \begin{bmatrix} d_{31} \\ d_{32} \end{bmatrix} \tag{10b}$$

where α_{11} and α_{22} are the thermal expansion coefficients in the longitudinal and transverse directions, d_{31} and d_{32} are piezoelectric strain constants of a single ply, and $\overline{Q}_{ij}$ are the transformed elastic constants, defined by

$$\begin{bmatrix} \overline{Q}_{11} \\ \overline{Q}_{12} \\ \overline{Q}_{22} \\ \overline{Q}_{16} \\ \overline{Q}_{26} \\ \overline{Q}_{66} \end{bmatrix} = \begin{bmatrix} c^4 & 2c^2s^2 & s^4 & 4c^2s^2 \\ c^2s^2 & c^4 + s^4 & c^2s^2 & -4c^2s^2 \\ s^4 & 2c^2s^2 & c^4 & 4c^2s^2 \\ c^3s & cs^3 - c^3s & -cs^3 & -2cs(c^2 - s^2) \\ cs^3 & c^3s - cs^3 & -c^3s & 2cs(c^2 - s^2) \\ c^2s^2 & -2c^2s^2 & c^2s^2 & (c^2 - s^2)^2 \end{bmatrix} \begin{bmatrix} Q_{11} \\ Q_{12} \\ Q_{22} \\ Q_{66} \end{bmatrix} \tag{11a}$$

$$\begin{bmatrix} \overline{Q}_{44} \\ \overline{Q}_{45} \\ \overline{Q}_{55} \end{bmatrix} = \begin{bmatrix} c^2 & s^2 \\ -cs & cs \\ s^2 & c^2 \end{bmatrix} \begin{bmatrix} Q_{44} \\ Q_{55} \end{bmatrix} \tag{11b}$$

where

$$Q_{11}=\frac{E_{11}}{(1-\nu_{12}\nu_{21})},\ \ Q_{22}=\frac{E_{22}}{(1-\nu_{12}\nu_{21})},\ \ Q_{12}=\frac{\nu_{21}E_{11}}{(1-\nu_{12}\nu_{21})},\ \ Q_{44}=G_{23},\ \ Q_{55}=G_{13},\ \ Q_{66}=G_{12} \tag{11c}$$

E_{11}, E_{22}, G_{12}, G_{13}, G_{23}, ν_{12} and ν_{21} have their usual meanings, and

$$c=\cos\theta,\quad s=\sin\theta \tag{11d}$$

where θ is the lamination angle with respect to the plate X-axis.

3. Analytical method and asymptotic solutions

Having developed the theory, we will try to solve Eqs. (1)–(4) with boundary conditions (5a)–(5h). Before proceeding, it is convenient first to define the following dimensionless quantities (with γ_{ijk} in Eq. (18) below are defined as in Shen (2000a,b))

$$\begin{aligned}
&x=\pi X/a,\ \ y=\pi Y/b,\ \ \beta=a/b,\ \ (W,W^*)=(\overline{W},\overline{W}^*)/[D_{11}^*D_{22}^*A_{11}^*A_{22}^*]^{1/4},\\
&F=\overline{F}/[D_{11}^*D_{22}^*]^{1/2},\ \ (\Psi_x,\Psi_y)=(\overline{\Psi}_x,\overline{\Psi}_y)a/\pi[D_{11}^*D_{22}^*A_{11}^*A_{22}^*]^{1/4},\\
&\gamma_{14}=\left[D_{22}^*/D_{11}^*\right]^{1/2},\ \ \gamma_{24}=\left[A_{11}^*/A_{22}^*\right]^{1/2},\ \ \gamma_5=-A_{12}^*/A_{22}^*,\\
&(\gamma_{31},\gamma_{41})=(a^2/\pi^2)\left[A_{55}-8D_{55}/t^2+16F_{55}/t^4,A_{44}-8D_{44}/t^2+16F_{44}/t^4\right]/D_{11}^*,\\
&(M_x,M_y,P_x,P_y)=(\overline{M}_x,\overline{M}_y,4\overline{P}_x/3t^2,4\overline{P}_y/3t^2)a^2/\pi^2D_{11}^*\left[D_{11}^*D_{22}^*A_{11}^*A_{22}^*\right]^{1/4},\\
&(\gamma_{T1},\gamma_{T2},\gamma_{P1},\gamma_{P2})=(A_x^T,A_y^T,B_x^P,B_y^P)a^2/\pi^2\left[D_{11}^*D_{22}^*\right]^{1/2},\\
&\lambda_x=Pb/4\pi^2\left[D_{11}^*D_{22}^*\right]^{1/2},\ \ (\delta_x,\delta_y)=(\Delta_x/a,\Delta_y/b)b^2/4\pi^2\left[D_{11}^*D_{22}^*A_{11}^*A_{22}^*\right]^{1/2}
\end{aligned} \tag{12}$$

Also let

$$\begin{bmatrix}A_x^T\\A_y^T\end{bmatrix}\Delta T=-\sum_{k=1}^{N}\int_{t_{k-1}}^{t_k}\begin{bmatrix}A_x\\A_y\end{bmatrix}_k\Delta T\,\mathrm{d}Z \tag{13a}$$

$$\begin{bmatrix}B_x^P\\B_y^P\end{bmatrix}\Delta V=-\sum_{k=1}^{N}\int_{t_{k-1}}^{t_k}\begin{bmatrix}B_x\\B_y\end{bmatrix}_k\frac{V_k}{t_k}\,\mathrm{d}Z \tag{13b}$$

The nonlinear Eqs. (1)–(4) may then be written in dimensionless form as

$$L_{11}(W)-L_{12}(\Psi_x)-L_{13}(\Psi_y)+\gamma_{14}L_{14}(F)=\gamma_{14}\beta^2L(W+W^*,F) \tag{14}$$

$$L_{21}(F)+\gamma_{24}L_{22}(\Psi_x)+\gamma_{24}L_{23}(\Psi_y)-\gamma_{24}L_{24}(W)=-\tfrac{1}{2}\gamma_{24}\beta^2L(W+2W^*,W) \tag{15}$$

$$L_{31}(W)+L_{32}(\Psi_x)-L_{33}(\Psi_y)+\gamma_{14}L_{34}(F)=0 \tag{16}$$

$$L_{41}(W)-L_{42}(\Psi_x)+L_{43}(\Psi_y)+\gamma_{14}L_{44}(F)=0 \tag{17}$$

where

$$
\begin{aligned}
L_{11}(\ ) &= \gamma_{110}\frac{\partial^4}{\partial x^4} + 2\gamma_{122}\beta^2\frac{\partial^4}{\partial x^2\,\partial y^2} + \gamma_{114}\beta^4\frac{\partial^4}{\partial y^4}\\
L_{12}(\ ) &= \gamma_{120}\frac{\partial^3}{\partial x^3} + \gamma_{112}\beta^2\frac{\partial^3}{\partial x\,\partial y^2}\\
L_{13}(\ ) &= \gamma_{131}\beta\frac{\partial^3}{\partial x^2\,\partial y} + \gamma_{133}\beta^3\frac{\partial^3}{\partial y^3}\\
L_{14}(\ ) &= \gamma_{141}\beta\frac{\partial^4}{\partial x^3\,\partial y} + \gamma_{143}\beta^3\frac{\partial^4}{\partial x\,\partial y^3}\\
L_{21}(\ ) &= \frac{\partial^4}{\partial x^4} + 2\gamma_{212}\beta^2\frac{\partial^4}{\partial x^2\,\partial y^2} + \gamma_{214}\beta^4\frac{\partial^4}{\partial y^4}\\
L_{22}(\ ) &= \gamma_{221}\beta\frac{\partial^3}{\partial x^2\,\partial y} + \gamma_{223}\beta^3\frac{\partial^3}{\partial y^3}\\
L_{23}(\ ) &= \gamma_{230}\frac{\partial^3}{\partial x^3} + \gamma_{232}\beta^2\frac{\partial^3}{\partial x\,\partial y^2}\\
L_{24}(\ ) &= \gamma_{241}\beta\frac{\partial^4}{\partial x^3\,\partial y} + \gamma_{243}\beta^3\frac{\partial^4}{\partial x\,\partial y^3}\\
L_{31}(\ ) &= \gamma_{31}\frac{\partial}{\partial x} + \gamma_{310}\frac{\partial^3}{\partial x^3} + \gamma_{312}\beta^2\frac{\partial^3}{\partial x\,\partial y^2}\\
L_{32}(\ ) &= \gamma_{31} - \gamma_{320}\frac{\partial^2}{\partial x^2} - \gamma_{322}\beta^2\frac{\partial^2}{\partial y^2}\\
L_{33}(\ ) &= \gamma_{331}\beta\frac{\partial^2}{\partial x\,\partial y}\\
L_{34}(\ ) &= L_{22}(\ )\\
L_{41}(\ ) &= \gamma_{41}\beta\frac{\partial}{\partial y} + \gamma_{411}\beta\frac{\partial^3}{\partial x^2\,\partial y} + \gamma_{413}\beta^3\frac{\partial^3}{\partial y^3}\\
L_{42}(\ ) &= L_{33}(\ )\\
L_{43}(\ ) &= \gamma_{41} - \gamma_{430}\frac{\partial^2}{\partial x^2} - \gamma_{432}\beta^2\frac{\partial^2}{\partial y^2}\\
L_{44}(\ ) &= L_{23}(\ )\\
L(\ ) &= \frac{\partial^2}{\partial x^2}\frac{\partial^2}{\partial y^2} - 2\frac{\partial^2}{\partial x\,\partial y}\frac{\partial^2}{\partial x\,\partial y} + \frac{\partial^2}{\partial y^2}\frac{\partial^2}{\partial x^2}
\end{aligned}
\tag{18}
$$

The boundary conditions expressed by Eqs. (5a)–(5h) become

$x = 0,\ \pi$:

$$W = \Psi_y = 0 \tag{19a}$$

$$F_{,xy} = M_x = P_x = 0 \tag{19b}$$

$$\frac{1}{\pi}\int_0^{\pi}\beta^2\frac{\partial^2 F}{\partial y^2}\,\mathrm{d}y + 4\lambda_x\beta^2 = 0 \tag{19c}$$

$y = 0,\ \pi$:

$$W = \Psi_x = 0 \tag{19d}$$

$$F_{,xy} = M_y = P_y = 0 \tag{19e}$$

$$\int_0^{\pi}\frac{\partial^2 F}{\partial x^2}\,\mathrm{d}x = 0 \text{ (movable edges)} \tag{19f}$$

$$\delta_y = 0 \text{ (immovable edges)} \tag{19g}$$

and the unit end-shortening relationships become:

$$\delta_x = -\frac{1}{4\pi^2\beta^2\gamma_{24}}\int_0^{\pi}\int_0^{\pi}\left\{\left[\gamma_{24}^2\beta^2\frac{\partial^2 F}{\partial y^2} - \gamma_5\frac{\partial^2 F}{\partial x^2} + \gamma_{24}\gamma_{223}\left(\beta\frac{\partial\Psi_x}{\partial y} + \frac{\partial\Psi_y}{\partial x}\right) - 2\gamma_{24}\gamma_{516}\beta\frac{\partial^2 W}{\partial x\,\partial y}\right] - \frac{1}{2}\gamma_{24}\left(\frac{\partial W}{\partial x}\right)^2 - \gamma_{24}\frac{\partial W}{\partial x}\frac{\partial W^*}{\partial x} + (\gamma_{24}^2\gamma_{T1} - \gamma_5\gamma_{T2})\Delta T + (\gamma_{24}^2\gamma_{P1} - \gamma_5\gamma_{P2})\Delta V\right\}\mathrm{d}x\,\mathrm{d}y \tag{20a}$$

$$\delta_y = -\frac{1}{4\pi^2\beta^2\gamma_{24}}\int_0^{\pi}\int_0^{\pi}\left\{\left[\frac{\partial^2 F}{\partial x^2} - \gamma_5\beta^2\frac{\partial^2 F}{\partial y^2} + \gamma_{24}\gamma_{230}\left(\beta\frac{\partial\Psi_x}{\partial y} + \frac{\partial\Psi_y}{\partial x}\right) - 2\gamma_{24}\gamma_{526}\beta\frac{\partial^2 W}{\partial x\,\partial y}\right] - \frac{1}{2}\gamma_{24}\beta^2\left(\frac{\partial W}{\partial y}\right)^2 - \gamma_{24}\beta^2\frac{\partial W}{\partial y}\frac{\partial W^*}{\partial y} + (\gamma_{T2} - \gamma_5\gamma_{T1})\Delta T + (\gamma_{P2} - \gamma_5\gamma_{P1})\Delta V\right\}\mathrm{d}y\,\mathrm{d}x \tag{20b}$$

By virtue of the fact that ΔV and ΔT are assumed to be uniform, the thermo-piezoelectric coupling in Eqs. (1)–(4) vanishes, but terms in ΔV and ΔT intervene in Eqs. (20a) and (20b).

Applying Eqs. (14)–(20b), the compressive postbuckling behavior of perfect and imperfect, shear deformable laminated plates with piezoelectric actuators under complex loading conditions is now determined by a perturbation technique. The essence of this procedure, in the present case, is to assume that

$$\begin{aligned} &W(x,y,\varepsilon) = \sum_{j=1}\varepsilon^j w_j(x,y),\quad F(x,y,\varepsilon) = \sum_{j=0}\varepsilon^j f_j(x,y),\\ &\Psi_x(x,y,\varepsilon) = \sum_{j=1}\varepsilon^j \psi_{xj}(x,y),\quad \Psi_y(x,y,\varepsilon) = \sum_{j=1}\varepsilon^j \psi_{yj}(x,y) \end{aligned} \tag{21}$$

where ε is a small perturbation parameter and the first term of $w_j(x,y)$ is assumed to have the form

$$w_1(x,y) = A_{11}^{(1)}\sin mx\sin ny \tag{22}$$

and the initial geometric imperfection is assumed to have a similar form

$$W^*(x,y,\varepsilon) = \varepsilon a_{11}^*\sin mx\sin ny = \varepsilon\mu A_{11}^{(1)}\sin mx\sin ny \tag{23}$$

where $\mu = a_{11}^*/A_{11}^{(1)}$ is the imperfection parameter.

Substituting Eq. (21) into Eqs. (14)–(17) and collecting the terms of the same order of ε, a set of perturbation equations is obtained. By using Eqs. (22) and (23) to solve these perturbation equations of each order, the amplitudes of the terms $w_j(x,y)$, $f_j(x,y)$, $\psi_{xj}(x,y)$ and $\psi_{yj}(x,y)$ are determined step by step. As a result, up to fourth-order asymptotic solutions can be obtained:

$$W = \varepsilon\left[A_{11}^{(1)}\sin mx\sin ny\right] + \varepsilon^3\left[A_{13}^{(3)}\sin mx\sin 3ny + A_{31}^{(3)}\sin 3mx\sin ny\right] + \varepsilon^4\left[A_{22}^{(4)}\sin 2mx\sin 2ny + A_{24}^{(4)}\sin 2mx\sin 4ny + A_{42}^{(4)}\sin 4mx\sin 2ny\right] + \mathrm{O}(\varepsilon^5) \tag{24}$$

$$F = -B_{00}^{(0)}\frac{y^2}{2} - b_{00}^{(0)}\frac{x^2}{2} + \varepsilon\left[B_{11}^{(1)}\cos mx\cos ny\right] + \varepsilon^2\left[-B_{00}^{(2)}\frac{y^2}{2} - b_{00}^{(2)}\frac{x^2}{2} + B_{20}^{(2)}\cos 2mx + B_{02}^{(2)}\cos 2ny\right] + \varepsilon^3\left[B_{13}^{(3)}\cos mx\cos 3ny + B_{31}^{(3)}\cos 3mx\cos ny\right] + \varepsilon^4\left[-B_{00}^{(4)}\frac{y^2}{2} - b_{00}^{(4)}\frac{x^2}{2} + B_{20}^{(4)}\cos 2mx + B_{02}^{(4)}\cos 2ny + B_{22}^{(4)}\cos 2mx\cos 2ny + B_{40}^{(4)}\cos 4mx + B_{04}^{(4)}\cos 4ny + B_{24}^{(4)}\cos 2mx\cos 4ny + B_{42}^{(4)}\cos 4mx\cos 2ny\right] + \mathrm{O}(\varepsilon^5) \tag{25}$$

$$\Psi_x = \varepsilon\left[C_{11}^{(1)}\cos mx\sin ny\right] + \varepsilon^2\left[C_{02}^{(2)}\sin 2ny\right] + \varepsilon^3\left[C_{13}^{(3)}\cos mx\sin 3ny + C_{31}^{(3)}\cos 3mx\sin ny\right] + \varepsilon^4\left[C_{02}^{(4)}\sin 2ny + C_{04}^{(4)}\sin 4ny + C_{22}^{(4)}\cos 2mx\sin 2ny + C_{24}^{(4)}\cos 2mx\sin 4ny + C_{42}^{(4)}\cos 4mx\sin 2ny\right] + \mathrm{O}(\varepsilon^5) \tag{26}$$

$$\Psi_y = \varepsilon\left[D_{11}^{(1)}\sin mx\cos ny\right] + \varepsilon^2\left[D_{20}^{(2)}\sin 2mx\right] + \varepsilon^3\left[D_{13}^{(3)}\sin mx\cos 3ny + D_{31}^{(3)}\sin 3mx\cos ny\right] + \varepsilon^4\left[D_{20}^{(4)}\sin 2mx + D_{40}^{(4)}\sin 4mx + D_{22}^{(4)}\sin 2mx\cos 2ny + D_{24}^{(4)}\sin 2mx\cos 4ny + D_{42}^{(4)}\sin 4mx\cos 2ny\right] + \mathrm{O}(\varepsilon^5) \tag{27}$$

It is mentioned that all coefficients in Eqs. (24)–(27) are related and can be written as functions of $A_{11}^{(1)}$ but, for the sake of brevity, the detailed expressions are not shown.

Next, substituting Eqs. (24)–(27) into the boundary conditions (19c) and (20a), the postbuckling equilibrium path can be written as

$$\lambda_x = \lambda_x^{(0)} + \lambda_x^{(2)}W_m^2 + \lambda_x^{(4)}W_m^4 + \cdots \tag{28}$$

and

$$\delta_x = \delta_x^{(0)} + \delta_x^{(2)}W_m^2 + \delta_x^{(4)}W_m^4 + \cdots \tag{29}$$

in which W_m is the dimensionless form of maximum deflection, which is assumed to be at the point $(x, y) = (\pi/2m, \pi/2n)$ and $\lambda_x^{(i)}$ and $\delta_x^{(i)}$ $(i = 0, 2, 4, \ldots)$ are given in detail in Appendix B.

Eqs. (28) and (29) can be employed to obtain numerical results for the postbuckling load-deflection or load-end-shortening curves of simply supported shear deformable composite laminated plates with piezoelectric actuators subjected to uniaxial compression combined with thermal and electric loads. From Appendix B, the buckling load of a perfect plate can readily be obtained numerically, by setting $\mu = 0$ (or $\overline{W}^*/t = 0$), while taking $W_m = 0$ (or $\overline{W}/t = 0$). In such a case, the minimum buckling load is determined by applying Eq. (28) for various values of the buckling mode (m, n), which determine the number of half-waves in the X- and Y-directions.

4. Numerical results and comments

To study the thermo-piezoelectric effects on the postbuckling behavior of shear deformable laminated plates, several numerical examples were solved for perfect and imperfect, symmetric cross-ply and anti-symmetric angle-ply laminated plates. Graphite/epoxy composite material and PZT-5A were selected for the substrate orthotropic layers and piezoelectric layers, respectively. The material properties for graphite/epoxy orthotropic layers of the substrate were (Oh et al., 2000): $E_{11} = 1.5 \times 10^5$ MN/m^2, $E_{22} = 9.0 \times 10^3$ MN/m^2, $G_{12} = G_{13} = 7.1 \times 10^3$ MN/m^2, $G_{23} = 2.5 \times 10^3$ MN/m^2, $v_{12} = 0.3$, $\alpha_{11} = 1.1 \times 10^{-6}(^\circ\text{C})^{-1}$, $\alpha_{22} = 25.2 \times 10^{-6}(^\circ\text{C})^{-1}$ and for PZT-5A piezoelectric layers $E_{11} = E_{22} = 6.3 \times 10^4$ MN/m^2, $G_{12} = G_{13} = G_{23} = 2.42 \times 10^4$ MN/m^2, $v_{12} = 0.3$, $\alpha_{11} = \alpha_{22} = 0.9 \times 10^{-6}(^\circ\text{C})^{-1}$ and $d_{31} = d_{32} = 2.54 \times 10^{-10}$ m/V. However, the analysis is equally applicable to other types of composite materials as well. For these examples (except for Figs. 1 and 2), the total thickness of the plate $t = 1.2$ mm whereas the thickness of piezoelectric layers is 0.1 mm, and all other orthotropic layers are of equal thickness.

As part of the validation of the present method, the postbuckling load-deflection curves for a perfect $(0_4)_T$ laminated square plate $(b/t = 20)$ subjected to uniaxial compression alone and under movable in-plane boundary conditions are compared in Fig. 1 with finite element method results of Sundaresan et al. (1996), using their material properties, i.e. $E_{11}/E_{22} = 25$, $G_{12}/E_{22} = G_{13}/E_{22} = 0.5$, $G_{23}/E_{22} = 0.2$, and $v_{12} = 0.25$. Moreover, the postbuckling load-deflection curves for perfect $(\pm 30_4)_T$ laminated square plates subjected to uniaxial compression alone and under immovable in-plane boundary conditions are compared in Fig. 2 with spline finite strip method results of Wang and Dawe (1999), using their material properties, i.e. $E_{11}/E_{22} = 40$, $G_{12}/E_{22} = G_{13}/E_{22} = 0.5$, $G_{23}/E_{22} = 0.6$, and $v_{12} = 0.25$. These two comparisons show that the results from the method presented agree well with the comparator solutions.

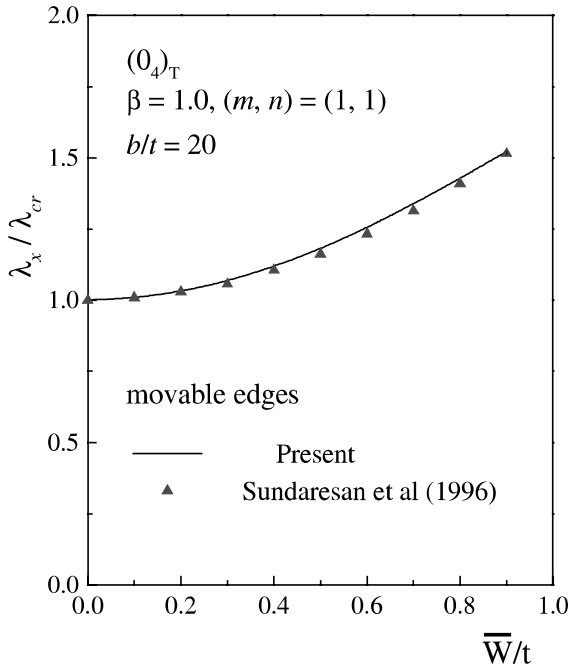

Fig. 1. Comparisons of postbuckling load-deflection curves for a $(0_4)_T$ laminated square plate under uniaxial compression.

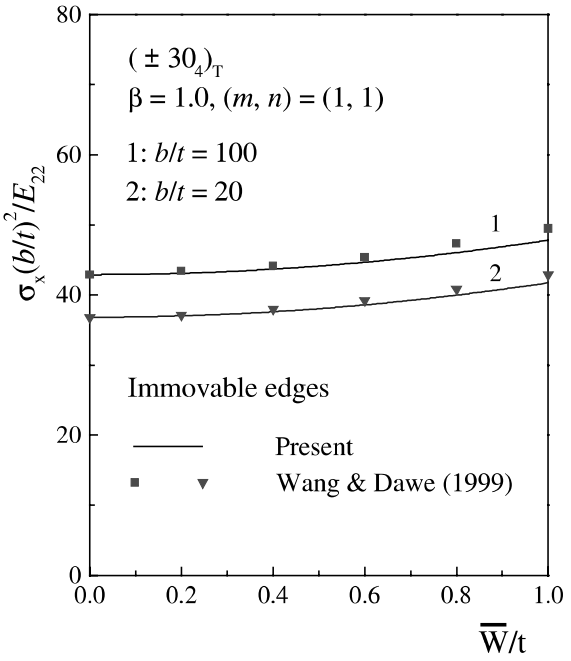

Fig. 2. Comparisons of postbuckling load-deflection curves for $(\pm 30_4)_T$ laminated square plates under uniaxial compression.

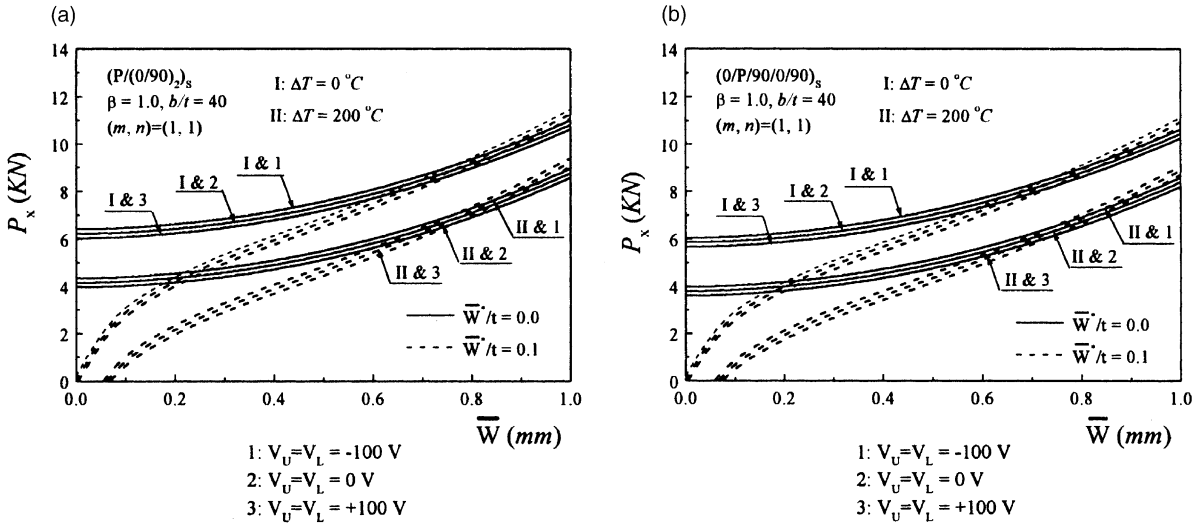

Fig. 3. Thermo-piezoelectric effects on the postbuckling load-deflection curves of laminated square plates: (a) $(P/(0/90)_2)_S$; (b) $(0/P/90/0/90)_S$.

A parametric study has been carried out and typical results are shown in Figs. 3–8. It should be appreciated that in all figures $\overline{W}^*/t$ denotes the dimensionless maximum initial geometric imperfection of the plate.

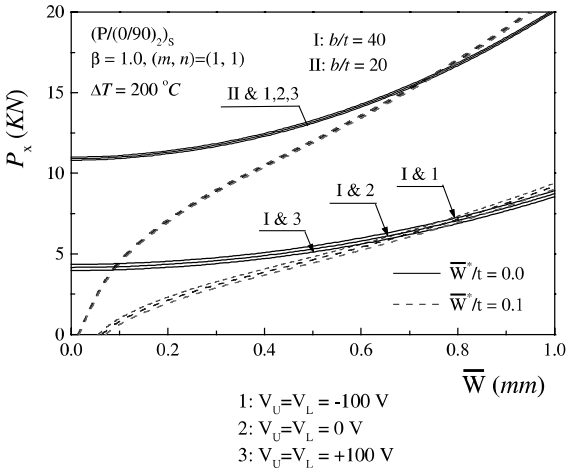

Fig. 4. Effect of plate thickness ratio b/t on the postbuckling of $(P/(0/90)_2)_S$ laminated square under complex loadings.

Fig. 3 gives the postbuckling load-deflection curves for a $(0/90)_{2S}$ symmetric cross-ply laminated square plates with symmetrically fully covered or embedded piezoelectric layers, referred to as $(P/(0/90)_2)_S$ and $(0/P/90/0/90)_S$, subjected to uniaxial compression and under immovable in-plane boundary conditions. Two thermal environmental conditions, referred to as I and II, are considered. For case I, $\Delta T = 0°C$ and for case II, $\Delta T = 200°C$. The control voltage with the same sign is also applied to both upper and lower piezoelectric layer, referred to as V_U and V_L. Three electric loading cases are considered. Here $V_U = V_L = 0$ V means the buckling under a grounding condition. It can be seen that the minus control voltages $V_U = V_L = -100$ V make the plate contract so that the buckling load is increased and the postbuckled deflection is decreased at the same temperature rise. In contrast, the plus control voltages $V_U = V_L = +100$ V decrease the buckling load and induce more large postbuckled deflections. It can also be seen that both buckling load and postbuckling strength are decreased with increase in temperature. Numerical results for some points on

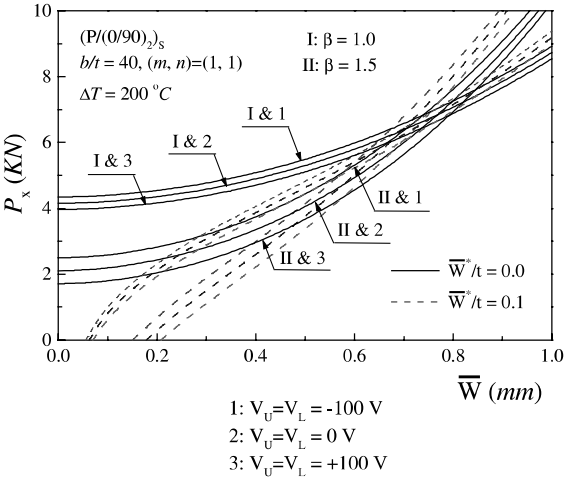

Fig. 5. Effect of plate aspect ratio on the postbuckling of $(P/(0/90)_2)_S$ laminated plates under environmental conditions.

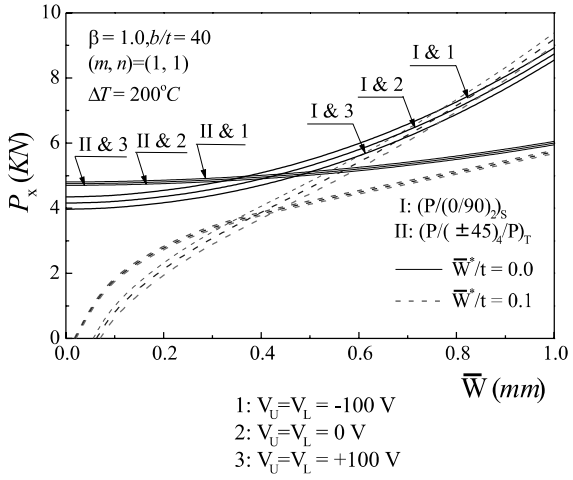

Fig. 6. Comparisons of postbuckling load-deflection curves of $(P/(0/90)_2)_S$ and $(P/(\pm 45)_4/P)_T$ laminated square plates under complex loadings.

the postbuckling curves for perfect $(P/(0/90)_2)_S$ and $(0/P/90/0/90)_S$ laminated square plates under complex loading conditions are presented in Tables 1 and 2 to enable easy comparisons by others in the future.

Fig. 4 gives the postbuckling load-deflection curves for $(P/(0/90)_2)_S$ laminated square plates with different width-to-thickness ratio b/t (=40 and 20) under environmental condition II and three electric loading cases. It can be found that the control voltage has a small effect on the postbuckling behavior of the plate with lower width-to-thickness ratio $b/t = 20$.

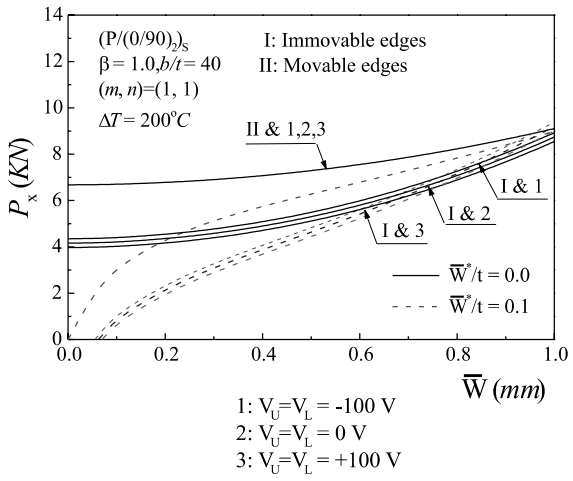

Fig. 7. Comparisons of postbuckling load-deflection curves for a $(P/(0/90)_2)_S$ laminated square plate under two cases of in-plane boundary conditions.

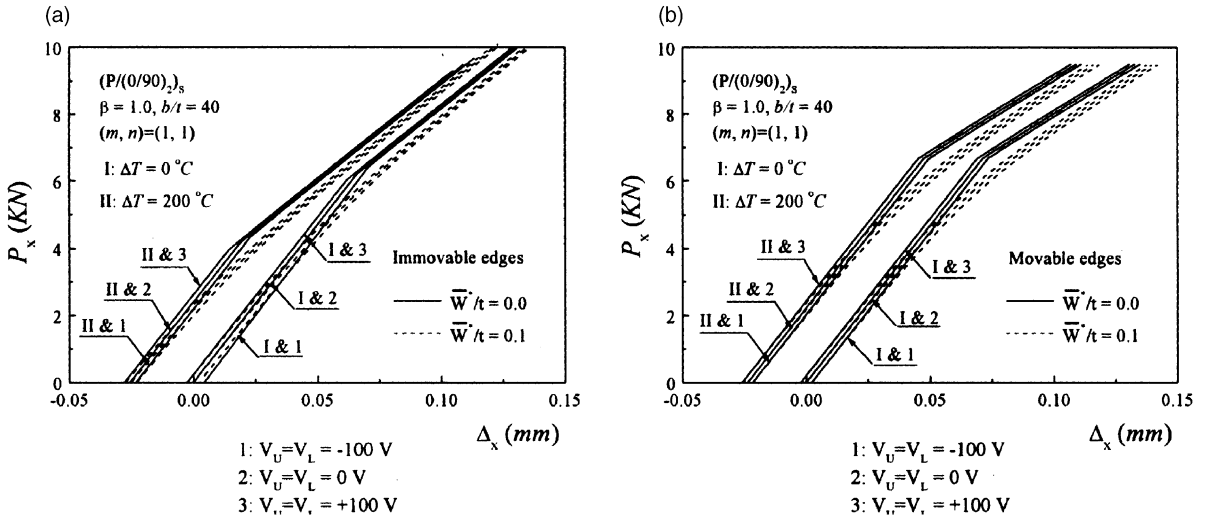

Fig. 8. Comparisons of postbuckling load-end-shortening curves for a $(P/(0/90)_2)_S$ laminated square plate under two cases of in-plane boundary conditions: (a) immovable edges; (b) movable edges.

Table 1
Comparisons of postbuckling loads $P_x(KN)$ for perfect $(P/(0/90)_2)_S$ piezolaminated square plates ($b/t = 40$) under uniform temperature rise and three sets of electric loading conditions

$\overline{W}$ (mm)	$\Delta T = 0$°C			$\Delta T = 200$°C		
	$V_U = V_L = -100$ V	$V_U = V_L = 0$ V	$V_U = V_L = +100$ V	$V_U = V_L = -100$ V	$V_U = V_L = 0$ V	$V_U = V_L = +100$ V
0	6.4100	6.2205	6.0310	4.3471	4.1576	3.9681
0.06	6.4261	6.2366	6.0471	4.3631	4.1736	3.9841
0.12	6.4744	6.2849	6.0954	4.4114	4.2219	4.0324
0.24	6.6677	6.4782	6.2887	4.6047	4.4152	4.2257
0.36	6.9905	6.8010	6.6115	4.9275	4.7380	4.5485
0.48	7.4440	7.2545	7.0650	5.3810	5.1915	5.0020
0.6	8.0297	7.8402	7.6507	5.9667	5.7772	5.5877
0.72	8.7495	8.5600	8.3705	6.6865	6.4970	6.3076
0.84	9.6059	9.4164	9.2269	7.5429	7.3534	7.1640
0.96	10.6016	10.4121	10.2226	8.5386	8.3492	8.1599
1.08	11.7400	11.5505	11.3610	9.6770	9.4876	9.2984

Fig. 5 shows the effect of plate aspect ratio β (=1.0 and 1.5) on the postbuckling behavior of $(P/(0/90)_2)_S$ laminated plates under environmental condition II and three electric loading cases. As expected, these results show that the buckling load and postbuckling strength are increased by decreasing plate aspect ratio β, with $\overline{W}/t < 0.8$. It can also be found that the effect of control voltage is more pronounced for the rectangular plate than for the square plate.

Fig. 6 compares the postbuckling load-deflection curves of $(0/90)_{2S}$ symmetric cross-ply and $(\pm 45_4)_T$ antisymmetric angle-ply laminated square plates with symmetrically fully covered piezoelectric layers under environmental condition II and three electric loading cases. It can be seen that the buckling load of the $(P/(0/90)_2)_S$ plate is lower than that of the $(P/(\pm 45)_4/P)_T$ plate, but the postbuckling load is higher when the deflection W is sufficiently large. It can also be found that the control voltage has a small effect on the postbuckling behavior of the $(P/(\pm 45)_4/P)_T$ plate.

Table 2
Comparisons of postbuckling loads P_x (KN) for perfect $(0/P/90/0/90)_S$ piezolaminated square plates ($b/t = 40$) under uniform temperature rise and three sets of electric loading conditions

$\overline{W}$ (mm)	$\Delta T = 0$°C			$\Delta T = 200$°C		
	$V_U = V_L = -100$ V	$V_U = V_L = 0$ V	$V_U = V_L = +100$ V	$V_U = V_L = -100$ V	$V_U = V_L = 0$ V	$V_U = V_L = +100$ V
0	6.0434	5.8539	5.6644	3.9804	3.7909	3.6014
0.06	6.0594	5.8699	5.6804	3.9964	3.8069	3.6174
0.12	6.1077	5.9182	5.7287	4.0447	3.8552	3.6657
0.24	6.3010	6.1115	5.9220	4.2380	4.0485	3.8590
0.36	6.6238	6.4343	6.2448	4.5608	4.3713	4.1818
0.48	7.0774	6.8879	6.6984	5.0143	4.8248	4.6352
0.6	7.6632	7.4737	7.2842	5.5999	5.4104	5.2208
0.72	8.3833	8.1938	8.0043	6.3196	6.1301	5.9405
0.84	9.2402	9.0507	8.8612	7.1757	6.9862	6.7965
0.96	10.2366	10.0471	9.8576	8.1711	7.9816	7.7918
1.08	11.3760	11.1864	10.9969	9.3090	9.1195	8.9294

Figs. 7 and 8 compare, respectively, the postbuckling load-deflection and load-end-shortening curves of a $(P/(0/90)_2)_S$ plate under two cases of the in-plane boundary conditions and under environmental condition II and three electric loading cases. It can be seen that the control voltage has no effect on the postbuckling load-deflection curves, but still has a significant effect on the postbuckling load-end-shortening curves of the plate under movable in-plane boundary condition. In contrast, the control voltages affect both load-deflection and load-end-shortening curves of the plate under immovable in-plane boundary condition.

The postbuckling load-deflection or load-end-shortening curves for imperfect shear deformable laminated plates have been plotted, along with the perfect plate results, in Figs. 3–8. In Figs. 3–6 the in-plane boundary condition is considered to be case (2), i.e. unloaded edges are immovable. In Figs. 3 and 5–8, the plate width-to-thickness ratio $b/t = 40$.

5. Concluding remarks

A postbuckling analysis has been presented for simply supported, shear deformable laminated plates with piezoelectric actuators subjected to the combined action of mechanical, electrical and thermal loads. The temperature field considered is assumed to be a uniform distribution over the plate surface and through the plate thickness and the electric field is assumed to be the transverse component E_Z only. The material properties are assumed to be independent of the temperature and the electric field. A perturbation technique is employed to determine the buckling loads and postbuckling equilibrium paths. The solutions presented give an insight into interaction between the mechanical, thermal and electric fields. Extensive parametric studies for symmetric cross-ply and antisymmetric angle-ply laminated plates with fully covered or embedded piezoelectric actuators subjected to complex loadings have been carried out. The results presented herein show that the minus control voltages increase the buckling load and decrease the postbuckled deflection at the same temperature rise, whereas the plus control voltages decrease the buckling load and induce more large postbuckled deflections for the plate with immovable unloaded edges. In contrast, for the plate with movable edges, the control voltage has no effect on the postbuckling load-deflection curves, but still has a significant effect on the postbuckling load-end-shortening curves of the plate. The results also confirm that the characteristics of postbuckling are significantly influenced by

temperature rise, the character of in-plane boundary conditions, transverse shear deformation, plate aspect ratio, fiber orientation and stacking sequence as well as initial geometric imperfections.

Acknowledgements

This work is supported in part by the National Natural Science Foundation of China under grant 59975058. The author is grateful for this financial support.

Appendix A

In Eqs. (1)–(4)

$$
\begin{aligned}
\widetilde{L}_{11}(\ ) &= \frac{4}{3t^2}\left[F_{11}^*\frac{\partial^4}{\partial X^4}+(F_{12}^*+F_{21}^*+4F_{66}^*)\frac{\partial^4}{\partial X^2\partial Y^2}+F_{22}^*\frac{\partial^4}{\partial Y^4}\right]\\
\widetilde{L}_{12}(\ ) &= \left[D_{11}^*-\frac{4}{3t^2}F_{11}^*\right]\frac{\partial^3}{\partial X^3}+\left[(D_{12}^*+2D_{66}^*)-\frac{4}{3t^2}(F_{12}^*+2F_{66}^*)\right]\frac{\partial^3}{\partial X\partial Y^2}\\
\widetilde{L}_{13}(\ ) &= \left[(D_{12}^*+2D_{66}^*)-\frac{4}{3t^2}(F_{21}^*+2F_{66}^*)\right]\frac{\partial^3}{\partial X^2\partial Y}+\left[D_{22}^*-\frac{4}{3t^2}F_{22}^*\right]\frac{\partial^3}{\partial Y^3}\\
\widetilde{L}_{14}(\ ) &= (2B_{26}^*-B_{61}^*)\frac{\partial^4}{\partial X^3\partial Y}+(2B_{16}^*-B_{62}^*)\frac{\partial^4}{\partial X\partial Y^3}\\
\widetilde{L}_{15}\left(\overline{N}^P\right) &= \frac{\partial^2}{\partial X^2}\left(B_{61}^*\overline{N}_{xy}^P\right)+2\frac{\partial^2}{\partial X\partial Y}\left(B_{16}^*\overline{N}_x^P+B_{26}^*\overline{N}_y^P\right)+\frac{\partial^2}{\partial Y^2}\left(B_{62}^*\overline{N}_{xy}^P\right)\\
\widetilde{L}_{16}\left(\overline{M}^P\right) &= \frac{\partial^2}{\partial X^2}\left(\overline{M}_x^P\right)+2\frac{\partial^2}{\partial X\partial Y}\left(\overline{M}_{xy}^P\right)+\frac{\partial^2}{\partial Y^2}\left(\overline{M}_y^P\right)\\
\widetilde{L}_{21}(\ ) &= A_{22}^*\frac{\partial^4}{\partial X^4}+(2A_{12}^*+A_{66}^*)\frac{\partial^4}{\partial X^2\partial Y^2}+A_{11}^*\frac{\partial^4}{\partial Y^4}\\
\widetilde{L}_{22}(\ ) &= \left[(B_{26}^*-B_{61}^*)-\frac{4}{3t^2}(E_{26}^*-E_{61}^*)\right]\frac{\partial^3}{\partial X^2\partial Y}+\left[B_{16}^*-\frac{4}{3t^2}E_{16}^*\right]\frac{\partial^3}{\partial Y^3}\\
\widetilde{L}_{23}(\ ) &= \left[B_{26}^*-\frac{4}{3t^2}E_{26}^*\right]\frac{\partial^3}{\partial X^3}+\left[(B_{16}^*-B_{62}^*)-\frac{4}{3t^2}(E_{16}^*-E_{62}^*)\right]\frac{\partial^3}{\partial X\partial Y^2}\\
\widetilde{L}_{24}(\ ) &= \frac{4}{3t^2}\left[(2E_{26}^*-E_{61}^*)\frac{\partial^4}{\partial X^3\partial Y}+(2E_{16}^*-E_{62}^*)\frac{\partial^4}{\partial X\partial Y^3}\right]\\
\widetilde{L}_{25}\left(\overline{N}^P\right) &= \frac{\partial^2}{\partial X^2}\left(A_{12}^*\overline{N}_x^P+A_{22}^*\overline{N}_y^P\right)+2\frac{\partial^2}{\partial X\partial Y}\left(-\frac{1}{2}A_{66}^*\overline{N}_{xy}^P\right)+\frac{\partial^2}{\partial Y^2}\left(A_{11}^*\overline{N}_x^P+A_{12}^*\overline{N}_y^P\right)
\end{aligned}
\tag{A.1}
$$

$$\widetilde{L}_{31}(\ ) = \left[A_{55} - \frac{8}{t^2}D_{55} + \frac{16}{t^4}F_{55}\right]\frac{\partial}{\partial X} + \frac{4}{3t^2}\left[\left(F^*_{11} - \frac{4}{3t^2}H^*_{11}\right)\frac{\partial^3}{\partial X^3} + \left((F^*_{21} + 2F^*_{66}) - \frac{4}{3t^2}(H^*_{12} + 2H^*_{66})\right)\frac{\partial^3}{\partial X\,\partial Y^2}\right]$$

$$\widetilde{L}_{32}(\ ) = \left[A_{55} - \frac{8}{t^2}D_{55} + \frac{16}{t^4}F_{55}\right] - \left[D^*_{11} - \frac{8}{3t^2}F^*_{11} + \frac{16}{9t^4}H^*_{11}\right]\frac{\partial^2}{\partial X^2} - \left[D^*_{66} - \frac{8}{3t^2}F^*_{66} + \frac{16}{9t^4}H^*_{66}\right]\frac{\partial^2}{\partial Y^2}$$

$$\widetilde{L}_{33}(\ ) = \left[(D^*_{12} + D^*_{66}) - \frac{4}{3t^2}(F^*_{12} + F^*_{21} + 2F^*_{66}) + \frac{16}{9t^4}(H^*_{12} + H^*_{66})\right]\frac{\partial^2}{\partial X\,\partial Y}$$

$$\widetilde{L}_{34}(\ ) = \widetilde{L}_{22}(\ )$$

$$\widetilde{L}_{35}\left(\overline{N}^P\right) = \frac{\partial}{\partial X}\left[\left(B^*_{61} - \frac{4}{3t^2}E^*_{61}\right)\overline{N}^P_{xy}\right] + \frac{\partial}{\partial Y}\left[\left(B^*_{16} - \frac{4}{3t^2}E^*_{16}\right)\overline{N}^P_{x} + \left(B^*_{26} - \frac{4}{3t^2}E^*_{26}\right)\overline{N}^P_{y}\right]$$

$$\widetilde{L}_{36}\left(\overline{S}^P\right) = \frac{\partial}{\partial X}\left(\overline{S}^P_{x}\right) + \frac{\partial}{\partial Y}\left(\overline{S}^P_{xy}\right)$$

$$\widetilde{L}_{41}(\ ) = \left[A_{44} - \frac{8}{t^2}D_{44} + \frac{16}{t^4}F_{44}\right]\frac{\partial}{\partial Y} + \frac{4}{3t^2}\left[\left((F^*_{12} + 2F^*_{66}) - \frac{4}{3t^2}(H^*_{12} + 2H^*_{66})\right)\frac{\partial^3}{\partial X^2\,\partial Y} + \left(F^*_{22} - \frac{4}{3t^2}H^*_{22}\right)\frac{\partial^3}{\partial Y^3}\right]$$

$$\widetilde{L}_{42}(\ ) = \widetilde{L}_{33}(\ )$$

$$\widetilde{L}_{43}(\ ) = \left[A_{44} - \frac{8}{t^2}D_{44} + \frac{16}{t^4}F_{44}\right] - \left[D^*_{66} - \frac{8}{3t^2}F^*_{66} + \frac{16}{9t^4}H^*_{66}\right]\frac{\partial^2}{\partial X^2} - \left[D^*_{22} - \frac{8}{3t^2}F^*_{22} + \frac{16}{9t^4}H^*_{22}\right]\frac{\partial^2}{\partial Y^2}$$

$$\widetilde{L}_{44}(\ ) = \widetilde{L}_{23}(\ )$$

$$\widetilde{L}_{45}\left(\overline{N}^P\right) = \frac{\partial}{\partial X}\left[\left(B^*_{16} - \frac{4}{3t^2}E^*_{16}\right)\overline{N}^P_{x} + \left(B^*_{26} - \frac{4}{3t^2}E^*_{26}\right)\overline{N}^P_{y}\right] + \frac{\partial}{\partial Y}\left[\left(B^*_{62} - \frac{4}{3t^2}E^*_{62}\right)\overline{N}^P_{xy}\right]$$

$$\widetilde{L}_{46}\left(\overline{S}^P\right) = \frac{\partial}{\partial X}\left(\overline{S}^P_{xy}\right) + \frac{\partial}{\partial Y}\left(\overline{S}^P_{y}\right)$$

$$\widetilde{L}(\ ) = \frac{\partial^2}{\partial X^2}\frac{\partial^2}{\partial Y^2} - 2\frac{\partial^2}{\partial X\,\partial Y}\frac{\partial^2}{\partial X\,\partial Y} + \frac{\partial^2}{\partial Y^2}\frac{\partial^2}{\partial X^2}$$

In the above equations $[A^*_{ij}]$, $[B^*_{ij}]$, $[D^*_{ij}]$, $[E^*_{ij}]$, $[F^*_{ij}]$ and $[H^*_{ij}]$ $(i,j = 1,2,6)$ are reduced stiffness matrices, defined as

$$\mathbf{A}^* = \mathbf{A}^{-1},\ \ \mathbf{B}^* = -\mathbf{A}^{-1}\mathbf{B},\ \ \mathbf{D}^* = \mathbf{D} - \mathbf{B}\mathbf{A}^{-1}\mathbf{B},\ \ \mathbf{E}^* = -\mathbf{A}^{-1}\mathbf{E},\ \ \mathbf{F}^* = \mathbf{F} - \mathbf{E}\mathbf{A}^{-1}\mathbf{B},$$
$$\mathbf{H}^* = \mathbf{H} - \mathbf{E}\mathbf{A}^{-1}\mathbf{E} \tag{A.2}$$

where A_{ij}, B_{ij} etc., are the plate stiffnesses, defined by

$$(A_{ij}, B_{ij}, D_{ij}, E_{ij}, F_{ij}, H_{ij}) = \sum_{k=1}^{N}\int_{t_{k-1}}^{t_k}(\overline{Q}_{ij})_k(1, Z, Z^2, Z^3, Z^4, Z^6)\,\mathrm{d}Z \quad (i,j = 1,2,6) \tag{A.3a}$$

$$(A_{ij}, D_{ij}, F_{ij}) = \sum_{k=1}^{N}\int_{t_{k-1}}^{t_k}(\overline{Q}_{ij})_k(1, Z^2, Z^4)\,\mathrm{d}Z \quad (i,j = 4,5) \tag{A.3b}$$

Appendix B

In Eqs. (28) and (29)

$$(\lambda_x^{(0)}, \lambda_x^{(2)}, \lambda_x^{(4)}) = \frac{1}{4\beta^2\gamma_{14}C_{11}}(S_0, S_2, S_4),\ \ \delta_x^{(0)} = C_{00}\lambda_x - \delta_x^P,\ \ \delta_x^{(2)} = \frac{1}{32\beta^2}C_{11}(1+2\mu),$$
$$\delta_x^{(4)} = \frac{1}{256\beta^2}\gamma_{14}\gamma_{24}C_{11}^2\left(\frac{m^4}{J_{13}\gamma_7} + \frac{n^4\beta^4}{J_{31}\gamma_6}\right)(1+\mu)^2(1+2\mu)^2 \tag{B.1}$$

in which (with g_{0j}, g_{13j} and g_{31j} $(j = 0, 1, \ldots, 8)$ are defined as in Shen (2000a,b))

$$S_0 = \Theta_{11}/(1+\mu) - S_0^P,\quad S_2 = \gamma_{14}\gamma_{24}\Theta_2(1+2\mu)/16,\quad S_4 = \gamma_{14}^2\gamma_{24}^2C_{11}(C_{24} - C_{44})/256,$$
$$\Theta_{11} = g_{08} + \gamma_{14}\gamma_{24}m^2n^2\beta^2\frac{g_{05}g_{07}}{g_{06}},\quad \Theta_2 = \left(\frac{m^4}{\gamma_7} + \frac{n^4\beta^4}{\gamma_6} + C_{22}\right)$$
$$\Theta_{13} = g_{138} + \gamma_{14}\gamma_{24}9m^2n^2\beta^2\frac{g_{135}g_{137}}{g_{136}},\quad \Theta_{31} = g_{318} + \gamma_{14}\gamma_{24}9m^2n^2\beta^2\frac{g_{315}g_{317}}{g_{316}}$$
$$\gamma_6 = 1 + \gamma_{14}\gamma_{24}\gamma_{230}^2\frac{4m^2}{\gamma_{41} + \gamma_{322}4m^2},\quad \gamma_7 = \gamma_{24}^2 + \gamma_{14}\gamma_{24}\gamma_{223}^2\frac{4n^2\beta^2}{\gamma_{31} + \gamma_{322}4n^2\beta^2} \tag{B.2}$$
$$C_{24} = 2(1+\mu)^2(1+2\mu)^2\Theta_2\left(\frac{m^4}{J_{13}\gamma_7} + \frac{n^4\beta^4}{J_{31}\gamma_6}\right),$$
$$C_{44} = (1+\mu)(1+2\mu)[2(1+\mu)^2 + (1+2\mu)]\left(\frac{m^8}{J_{13}\gamma_7^2} + \frac{n^8\beta^8}{J_{31}\gamma_6^2}\right)$$
$$J_{13} = \Theta_{13}C_{11}(1+\mu) - \Theta_{11}C_{13} + J^P,\quad J_{31} = \Theta_{31}C_{11}(1+\mu) - \Theta_{11}C_{31} - J^P$$

in the above equations, for the case of four edges movable

$$C_{00} = \gamma_{24},\ \ C_{11} = C_{13} = m^2,\ \ C_{31} = 9m^2,\ \ C_{22} = 0,\ \ S_0^P = J^P = 0,$$
$$\delta_x^P = \frac{1}{4\beta^2\gamma_{24}}[(\gamma_{24}^2\gamma_{T1} - \gamma_5\gamma_{T2})\Delta T + (\gamma_{24}^2\gamma_{P1} - \gamma_5\gamma_{P2})\Delta V] \tag{B.3}$$

and for the case of unloaded edges immovable

$$C_{00} = (\gamma_{24}^2 - \gamma_5^2)/\gamma_{24},\ \ C_{11} = m^2 + \gamma_5n^2\beta^2,\ \ C_{13} = m^2 + 9\gamma_5n^2\beta^2,$$
$$C_{31} = 9m^2 + \gamma_5n^2\beta^2,\ \ C_{22} = 2n^4\beta^4,$$
$$S_0^P = \gamma_{14}n^2\beta^2[(\gamma_{T2} - \gamma_5\gamma_{T1})\Delta T + (\gamma_{P2} - \gamma_5\gamma_{P1})\Delta V],$$
$$\delta_x^P = \frac{C_{00}}{4\beta^2}(\gamma_{T1}\Delta T + \gamma_{P1}\Delta V),$$
$$J^P = 8\gamma_{14}m^2n^2\beta^2(1+\mu)[(\gamma_{T2} - \gamma_5\gamma_{T1})\Delta T + (\gamma_{P2} - \gamma_5\gamma_{P1})\Delta V]. \tag{B.4}$$

References

Argyris, J., Tenek, L., 1995. Postbuckling of composite laminates under compressive load and temperature. Comput. Meth. Appl. Mech. Engng. 128, 49–80.

Icardi, U., Di Sciuva, M., 1996. Large-deflection and stress analysis of multilayered plates with induced-strain actuators. Smart Mater. Struct. 5, 140–164.

Ishihara, M., Noda, N., 2000. Piezothermoelastic analysis of a cross-ply laminate considering the effects of transverse shear and coupling. J. Therm. Stresses 23, 441–461.

Jonnalagadda, K.D., Blandford, G.E., Tauchert, T.R., 1994. Piezothermoelastic composite plate analysis using first-order shear deformation theory. Comput. Struct. 51, 79–89.

Kapuria, S., Dube, G.P., Dumir, P.C., Sengupta, S., 1997. Levy-type piezothermoelastic solution for hybrid plate by using first-order shear deformation theory. Composites Part B 28, 535–546.

Lee, H.J., Saravanos, O.A., 1997. Generalized finite element formulation for smart multilayered thermal piezoelectric composite plates. Int. J. Solids Struct. 34, 3355–3371.

Librescu, L., Lin, W., Nemeth, M.P., Starnes, J.H., 1995. Thermomechanical postbuckling of geometrically imperfect flat and curved panels taking into account tangential edge constraints. J. Therm. Stresses 18, 465–482.

Librescu, L., Souza, M.A., 1993. Post-buckling of geometrically imperfect shear-deformable flat panels under combined thermal and compressive edge loadings. ASME J. Appl. Mech. 60, 526–533.

Librescu, L., Stein, M., 1991. A geometrically nonlinear theory of transversely isotropic laminated composite plates and its use in the post-buckling analysis. Thin-Walled Struct. 11, 177–201.

Noor, A.K., Peters, J.M., 1992. Postbuckling of multilayered composite plates subjected to combined axial and thermal loads. Finite Elements Anal. Des. 11, 91–104.

Noor, A.K., Peters, J.M., 1994. Finite element buckling and postbuckling solutions for multilayered composite panels. Finite Elements Anal. Des. 15, 343–367.

Noor, A.K., Starnes, J.H., Peters, J.M., 1993. Thermomechanical buckling and postbuckling of multilayered composite panels. Compos. Struct. 23, 233–251.

Oh, I.K., Han, J.H., Lee, I., 2000. Postbuckling and vibration characteristics of piezolaminated composite plate subjected to thermo-piezoelectric loads. J. Sound Vib. 233, 19–40.

Reddy, J.N., 1984. A simple higher-order theory for laminated composite plates. ASME J. Appl. Mech. 51, 745–752.

Reddy, J.N., 1999. On laminated composite plates with integrated sensors and actuators. Engng. Struct. 21, 568–593.

Shen, H.S., Zhang, J.W., 1988. Perturbation analyses for the postbuckling of simply supported rectangular plates under uniaxial compression. Appl. Math. Mech. 9, 793–804.

Shen, H.S., 1988. Thermomechanical post-buckling analysis of imperfect laminated plates using a higher-order shear-deformation theory. Comput. Struct. 66, 395–409.

Shen, H.S., 2000a. Postbuckling of shear deformable laminated plates under biaxial compression and lateral pressure and resting on elastic foundations. Int. J. Mech. Sci. 42, 1171–1195.

Shen, H.S., 2000b. Postbuckling analysis of shear deformable laminated plates on two-parameter elastic foundations. Mech. Compos. Mater. Struct. 7, 249–268.

Shen, H.S., 2000c. Thermomechanical postbuckling of imperfect shear deformable laminated plates on elastic foundations. Comput. Meth. Appl. Mech. Engng. 189, 761–784.

Sundaresan, P., Singh, G., Rao, G.V., 1996. Buckling and postbuckling analysis of moderately thick laminated rectangular plates. Comput. Struct. 61, 79–86.

Tauchert, T.R., 1992. Piezothermalelastic behavior of a laminated plate. J. Therm. Stresses 15, 25–37.

Wang, S., Dawe, D.J., 1999. Spline FSM postbuckling analysis of shear deformable rectangular laminates. Thin-Walled Struct. 34, 163–178.

Xu, K., Noor, A.K., Tang, Y.Y., 1995. Three-dimensional solutions for coupled thermoelectroelastic response of multilayered plates. Comput. Meth. Appl. Mech. Engng. 126, 355–371.